Somatic PI3K activity regulates transition to the spermatocyte stages in *Drosophila* testis

SAMIR GUPTA and KRISHANU RAY*

Department of Biological Sciences, Tata Institute of Fundamental Research, Mumbai 400 005, India

**Corresponding author (Email, krishanu@tifr.res.in; krishanu64@gmail.com)*

Spermatogenesis, involving multiple transit amplification divisions and meiosis, occurs within an enclosure formed by two somatic cells. As the cohort of germline cells divide and grow, the surface areas of the somatic cells expand maintaining a tight encapsulation throughout the developmental period. Correlation between the somatic cell growth and germline development is unclear. Here, we report standardization of a quantitative assay developed for estimating the somatic roles of target molecules on germline division and differentiation in *Drosophila* testis. Using the assay, we studied the somatic roles of phosphatidylinositol-3-kinase (PI3K). It revealed that the expression of $PI3K^{DN}$ is likely to facilitate the early germline development at all stages, and an increase in the somatic PI3K activity during the early stages delays the transition to spermatocyte stage. Together, these results suggest that somatic cell growth plays an important role in regulating the rate of germline development.

[Gupta S and Ray K 2017 Somatic PI3K activity regulates transition to the spermatocyte stages in *Drosophila* testis. *J. Biosci.* **42** 285–297]

1. Introduction

Stem cell progeny undergoes different extents of transit amplification divisions before differentiation, which is at the core of tissue growth during development and regeneration. The transit amplification process is regulated through a continuous cross-talk between the developing tissue and the differentiated cells around it. Various cell signalling systems, primarily driven by the epidermal growth factor (EGF) and the insulin-like growth factor (IGF) families, control the tissue homeostasis (Biteau *et al.* 2011; Wu and Hill 2009). Dysregulation of the process may result in tumorigenesis (Breuhahn *et al.* 2006). *Drosophila* testis has emerged an ideal system for correlating the physiological outcome of cell signalling to the morphogenetic changes observed in the adjacent cells (Fuller 1993). It harbours two types of stem cell populations, the germline stem cells (GSCs) and the somatic cyst stem cells (CySCs), that are physically attached to a set of terminally differentiated somatic cells, called the hub, at the apical end of the testis (Hardy *et al.* 1979). A gonialblast, formed through an asymmetric division of a GSC, is encapsulated by two somatic cyst cells derived from two adjacent CySCs. Together, they form a spermatogonial cyst. The gonialblast then undergoes four rounds of synchronized mitosis within the somatic enclosure, producing a 16-cell spermatogonial cyst, which differentiates into a 16-cell spermatocyte cyst (Fuller 1993). The spermatogonia to spermatocyte transition is associated with distinct decompaction of chromatin in the germline cells during the S1–S3 stages (Cenci *et al.* 1994), and the germline-specific expression of the *spermatocyte-arrest* (*sa*) gene from the S3 stage onward (Lin *et al.* 1996). The entire process involves extensive germ-soma cross talk (Gao and Liu 2012; Zoller and Schulz 2012).

The size of each germline cell increases slightly during the transit amplification divisions (Insco *et al.* 2009). Thus, the volume occupied by the germline cells within a cyst increases more than two folds after each mitosis. The somatic cyst cells maintain a tight enclosure around each germline cell within a cyst during this stage, which is construed to be

Keywords. *Drosophila*; phosphatidylinositol-3-kinase (PI3K); somatic cyst cell; spermatocyte; *spermatocyte-arrest*; testis; *traffic-jam*

Supplementary materials pertaining to this article are available on the Journal of Biosciences Website.

DOI: 10.1007/s12038-017-9678-5

Published online: 22 April 2017

critical for the progression of spermatogonial division and differentiation (Lim and Fuller 2012; Zoller and Schulz 2012). A breach in the somatic encapsulation due to the loss of somatic cyst cells or the disruption of septate junctions between the cyst cells disrupts transit amplification divisions and subsequent differentiation, resulting in an abnormal accumulation of undifferentiated germ cells in the testis (Lim and Fuller 2012; Fairchild *et al.* 2015). Therefore, it is essential that the size of the somatic cyst cells, particularly the surface areas of the cells, grows in synchrony maintaining the enclosure. Numerous reports have suggested that the activation of the phosphatidylinositol-3-kinase (PI3K), Akt, and mechanistic Target Of Rapamycin Complex 1 (mTORC1) downstream to the growth factor receptor activation leads to cell growth and proliferation (Leevers *et al.* 1996; Weinkove *et al.* 1999; Ferreira and Milán 2015; Soler *et al.* 2015; Salony *et al.* 2016). In *Drosophila* testis, the Epidermal Growth Factor Receptor (EGFR) signalling in the somatic cyst cells plays an important role in terminating the transit amplification divisions (Fuller 1998; Kiger *et al.* 2000; Tran *et al.* 2000; Davies and Fuller 2008). However, the link between the PI3K and EGFR signalling in this process is not known.

Here, we report standardization of a quantitative genetic screen for identifying the somatic requirements of the functions of various candidate molecules in regulating the germline transit amplification. We used this assay to explore the somatic requirements of PI3K in regulating the germline divisions and differentiations. The results show that the PI3K activity in the somatic cyst cells plays a significant role in controlling the transition to the S3 spermatocyte stage after the conclusion of transit amplification divisions. Altogether, the data highlights a possible role of the somatic inositide signalling cascade in regulating the development and differentiation of the neighboring germ cells.

2. Material and methods

2.1 *Drosophila stocks and culture condition*

Fly stocks (supplementary table 1) and crosses were maintained on standard *Drosophila* medium at 25°C. The flies were grown for four days at 29°C before dissection and fixation as described before (Joti *et al*. 2011).

2.2 *Whole mount immuno-staining*

Testes from a four-day-old male were dissected and fixed in 4% paraformaldehyde for 1 hour at room temperature. The tissue was washed 3 times in 0.3% TritonX100 in phosphate-buffered-saline (PTX) then incubated with an appropriate dilution of primary antibodies (1:4000 α-phospho-Histone-3, 1:100 α-Armadillo, 1:50 α-Vasa, 1:100 α-BrdU, and 1:10000 α-Traffic-jam) for overnight, followed by washing in PTX, 2 h incubation at room temperature with Alexa dye-conjugated secondary antibodies (Invitrogen) at 1:400 dilution in PTX, and a final set of wash in PTX. For BrdU staining the dissected testes were incubated with 10 µg/mL, BrdU followed by paraformaldehyde fixation in 0.2M NaOH, followed by the antibody staining. For Golgi visualization, the testes were stained with Alexa-Fluor-594 conjugated Wheat Germ Agglutinin (Invitrogen) and costained with 0.001% Hoechst-33342 (Sigma Chemical Co. USA), then washed in PTX for 3 times, and mounted with a drop of Vectashield® (Vector Laboratory Inc., USA).

2.3 *Image acquisition, analysis, and cyst profile quantification*

All images were acquired using Olympus FV1000SPD laser scanning confocal microscope using 10X, 0.3 NA and 60X, 1.35 NA objectives. Multiple optical slices were collected covering the entire apical part of the testes. The images were analyzed using ImageJ® (*http://fiji.sc/Fiji*). The Cell-counter™ plugin was used for counting the stained nuclei. For estimating the germ-soma ratio, all the Hoechst-stained, as well as the Histone-RFP-marked nuclei, present in the apical ~100 µm region of the testes were counted. The *tjGal4>UAS-His2A-RFP* marked all the somatic cyst nuclei in this region. A subtraction of the number of HisRFP marked nuclei from that of the total Hoechst stained nuclei provided an estimate of the pool consisting of mostly the germline cells in this region (supplementary figure 1). The somatic knockdown of *ddlc1* and other dynein subunits is known to induce germline hyperproliferation (Joti *et al.* 2011). It was used as a positive control to test the efficacy of the assay. Aberrant transit amplification divisions are likely to result in the relative expansion or reduction of the germline population within each cyst encapsulated by two somatic cyst cells. Hence, the ratio between the number of somatic cyst cells and the total nuclei present at the testis apex would either increase or decrease according to the alteration of the extent and rates of cell cycles within each cyst. The results obtained from the *ddlc1* (LC8 subunit of Dynein) and *Dhc64C* (Dynein heavy chain) were consistent with this conjecture (supplementary figure 1).

It is to be noted that an increase in the number of germline cells within cysts, somatic cells beyond the *tjGal4* expression stage, or loss of *tjGal4* expression, would increase the germ/soma ratio. Also, the ratio could be increased due to a premature and selective loss of the somatic cyst cells, or accumulation of the post transit-amplification stage cysts at the testis apex. However, the assay provided a significant quantitative advantage over the currently used empirical methods as the first level screen. Therefore, to determine

actual defect, we deployed secondary screens. We immunostained testes carrying *vasa-GFP tjGal4>UAS-His2ARFP/+* in the background with Armadillo to estimate the cyst profile, quantified the M-phase index by anti-PH3 staining, and estimated cyst profiles in the *BampbmpGFP* (marking the bam-expressing germline) and *sa-mCD8-GFP* (marking spermatocytes from the S3 stage) backgrounds, respectively.

3. Results

3.1 *Germline differentiation is marked by characteristic chromatin decondensation*

The spermatogonial nuclei have tightly packed chromatin, which is easily recognized by the relatively higher intensity of staining with the DNA markers such as DAPI and the Hoechst dye (figure 1A). The chromatin packing, indicated by the lowered Hoechst-staining intensity, is progressively dispersed with an associated increase in the nuclei size during the transition through the spermatocyte stages (figure 1A). The spermatogonial development from 4-8 cell stages is defined by the expression of *bag-of-marbles* (*bam*), which appears in the germline at the four-cell stage and disappears soon after the division of the eight-cell cyst (figure 1B) (Insco *et al.* 2009). The initiation of *bam* expression is critical for the termination of spermatogonial divisions at the 16-cell stage, and its elimination from the spermatogonial cells mark the transition to the spermatocyte stage (Insco *et al.* 2009). The somatic cyst cells express a transcription co-factor, *traffic-jam* (*tj,* Li *et al.* 2003) throughout the spermatogonial stages and until the S2 spermatocyte stage (arrowhead, figure 1B and C). Hoechst-staining of the whole testis revealed progressive decondensation of chromatin in the germline cells as the cyst progressed through the spermatocyte stages (figure 1A and D).

Consistent with the previous results (Cenci *et al.* 1994), we also found that the one-hour pulse labeling of BrdU, which is an indicator of the S-phase, and the phospho-Histone-3 (PH3) immunostaining, marking the M-phase nuclei, always labeled the spermatogonial nuclei containing condensed chromatin (figure 1E–F; supplementary figure 1). Therefore, an empirical inspection of the proportion of the intense, Hoechst-stained nuclei at the testis apex has been used to estimate the germline over-proliferation in adult testis (Kiger *et al.* 2000; Tran *et al.* 2000). Most of these studies have been conducted in eight days or older adults, a considerably late stage in the life cycle of *Drosophila*. Although such as an assay is useful for a quick identification of obvious defects, it is inadequate for identifying relatively small but statistically significant changes.

Therefore, to determine the somatic factors influencing the germline divisions, we expressed various UAS-linked transgenes, containing either dominant negative, constitutively active or dsRNA constructs, using the *traffic-jam-Gal4* (*tjGal4*) driver, and estimated the somatic and germline populations at the apical region of testes of 4-days-old adults. Tj is exclusively expressed in the cyst stem cells and the somatic cyst cells during the transit amplification stages (Li *et al.* 2003). The expression continues until the early 16-cell spermatocyte stage. Hence, the assay allowed us to estimate quantitatively and compare the cell non-autonomous effects on germ cell proliferation caused by the somatic perturbations of various factors during the early stages.

3.2 *Somatic PI3K activity is essential for proper development of the neighbouring germline cells*

The germ cell proliferation is regulated by both germ cell-intrinsic and extrinsic factors. Germline-intrinsic factors such as the Bag-of-marbles (Bam) and Benign-gonial-cell-neoplasia (Bgcn) (Gönczy *et al*. 1997; Insco *et al*. 2009; Li *et al*. 2009), along with the EGFR signalling in the somatic cyst cells have been reported to play essential roles in regulating the spermatogonial divisions and differentiation (Davies and Fuller 2008; Fuller 1998; Kiger *et al.* 2000; Tran *et al.* 2000). In mammalian cells, EGFR also activates type IA PI3K regulating the downstream signaling (Kusumi *et al*. 2007; Tétreault *et al*. 2008; Toulany *et al*. 2007; Duan *et al*. 2014). *Drosophila* genome carries only one type I PI3K catalytic subunit. It is encoded by the Pi3K92E gene which expresses in a variety of tissues (Leevers *et al*. 1996; Xi *et al*. 2014). PI3K activation is associated with both cell growth (Galagovsky *et al*. 2014; Ibar *et al*. 2013) and proliferation control (Kasahara *et al*. 2013). All these cellular functions of PI3K are described as cell autonomous. In comparison, little is known about the neighborhood effects of PI3K-dependent signalling within a tissue.

The somatic expression of $Pi3K92E^{dsRNA}$ (figure 2A) and $Pi3K68D^{dsRNA}$ (figure 2B) did not cause visible accumulation of early spermatogonial cells at the testis apex, whereas the expression of $Pi3K92E^{A2860C}$ ($PI3K^{DN}$) restricted the area occupied by the spermatogonial pool at the testis apex (figure 2C). The somatic expression of $Pi3K92E^{CAAX}$ ($PI3K^{CA}$) (figure 2D), $Ras^{V12,\ C40}$ (figure 2E), and $PTEN^{dsRNA}$ (figure 2F), respectively, bloated the tip of the testis. The defect was most prominent in the $PI3K^{CA}$ background (supplementary figure 2B). The expression of $Ras^{V12,\ C40}$ selectively activates the PI3K *in vivo* (Halfar *et al*. 2001; Karim and Rubin 1998), and the PTEN knockdown would enhance the PI3K-depednent signalling by reducing the PI(3,4,5)P de-phosphorylation (Lee *et al*. 1999).

Further analysis of the data highlighted subtle quantitative differences amongst the defects (table 1 and figure 2G). The somatic expression of $Pi3K92E^{dsRNA}$ and $PTEN^{dsRNA}$ caused no significant change in the germ/soma ratios (figure 2H), though the expression of the transgenes using a ubiquitous, *actinGal4* driver caused wide-spread

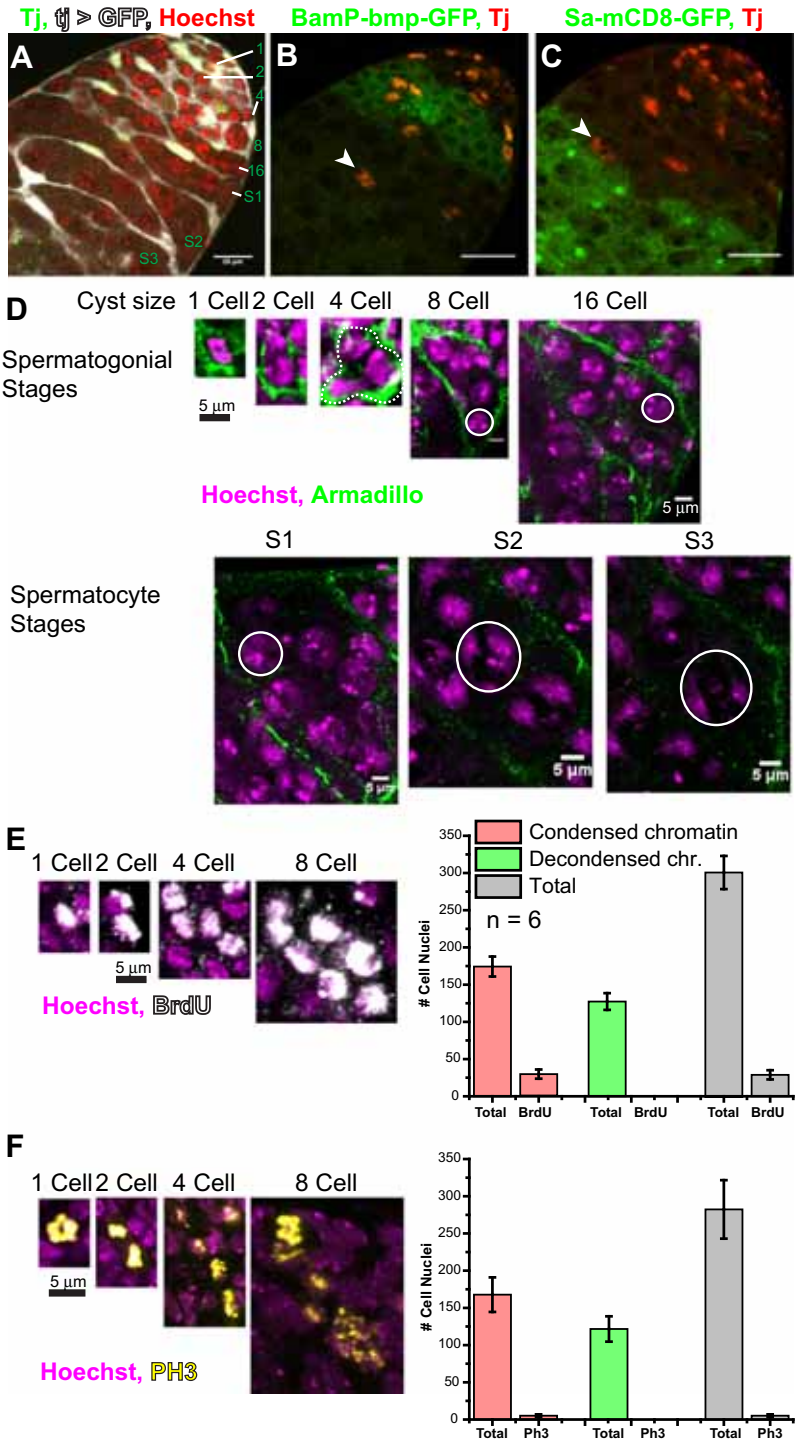

Figure 1. Chromatin morphology of early germline cells in adult *Drosophila* testis. (**A**) Apical tip of a *tjGal4; UAS-GFP* testis stained with α-Tj, and the Hoechst dye, marking the nuclei (Tj, green) and cytoplasm (GFP, white) of somatic cyst cells, as well as all nuclei (red). 1–16 cell spermatogonial stages, and the early spermatocyte (S1–S3) stages, are marked on the panel. *BamP-bmp-GFP* (**B**) and *sa-mCD8GFP* (**C**) testes stained with α-Tj (red). Arrowheads mark the terminal Tj-expressing cyst nuclei. (**D**) Cropped images of control testis stained with α-armadillo (green) and the Hoechst dye (magenta), highlighting the spermatogonial and early spermatocyte stages. Cropped images of BrdU-stained (white, **E**) and α-PH3 stained (yellow, **F**) clusters of germ cells. Histograms depict an average number of condensed, decondensed and total nuclei estimated from wild-type control, and the BrdU/PH3-stained fractions. No decondensed nuclei were found to be BrDU or PH3 positive. All error bars depict ±SD, and the pair-wise significance of differences (p-values, *<0.05, **<0.01, and ***<0.001) were estimated using unpaired Student's T-test and Mann-Whitney μ-test.

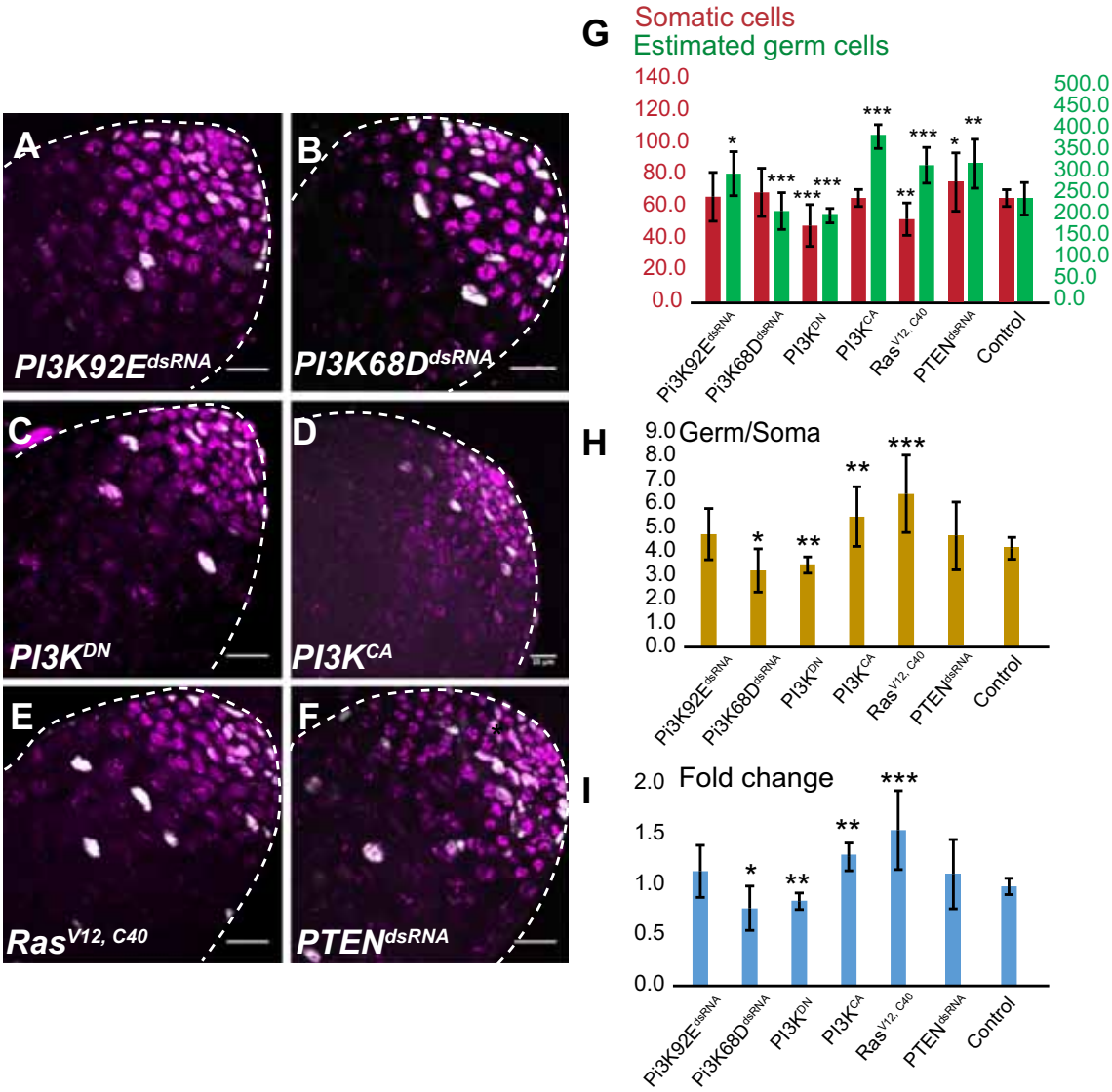

Figure 2. Estimation of the germ/soma ratios at the testis apex cause by the somatic perturbation of PI3K functions. (**A–F**) *tjGal4 UAS-His2A-RFP* testes expressing different transgenic elements as indicated on the panels were stained with the Hoechst dye (magenta) and the *tjGal4>UAS-His2A-RFP* expression marked the somatic cyst cells (white). Broken white lines mark the testes boundaries and scale bars indicate 20 µm. (**G–I**) Histograms depict the average number of somatic (red) and germline cells (green) within the ROI (**G**), the distribution of germ/soma ratios (**H**) and the fold change (**I**) in different genetic backgrounds, and error bars depict ±SD. The pair-wise significance of differences (p-values, *<0.05, **<0.01, and *** <0.001) relative to appropriate wild-type controls were calculated using the Student's t-test and Mann-Whitney µ-test.

embryonic lethality. The apparent difference in phenotypes between the somatic expressions of $Pi3K92E^{dsRNA}$ and $PI3K^{DN}$ may suggest some redundancy amongst the PI3K activities or reduced efficacy of the RNAi induced by the reagents. To test the first conjecture, we expressed the $Pi3K68D^{dsRNA}$ (type II). Similar to the expressions of $PI3K^{DN}$, it reduced the germ/soma ratio marginally (figure 2H). On the other hand, the expression of $PTEN^{dsRNA}$ increased both the somatic and germline populations. As a result, the germ-soma ratio remained unaltered (figure 2H). The fold change analysis further indicated that the loss of somatic PI3K activity could increase the proportion of cysts containing fewer germ cells (figure 2I), whereas increasing the PI3K activity would accumulate cysts containing a relatively higher number of germ cells. Hence, the level of PI3K activity in early stage somatic cells appeared to regulate the spermatogonial development and differentiation.

Table 1. Estimation of the total, somatic and the germ cell nuclei at the apical tip of adult testis expressing different UAS-transgenes in the *tjGal4>UAS-HisRFP* background

Transgene	Total Avg.± S.D.	Germ Avg. ± S.D.	Somatic Avg.± S.D.	n
Control	324.4 ± 27.8	261 ± 24.8	63.6 ± 5.1	21
PI3K92E dsRNA	351.7 ± 75.7	285.3 ± 58	66.4 ± 18.8	7
PI3K68D dsRNA	271 ± 49.7	206.5 ± 41.1	64.5 ± 17.7	15
PI3K (DN)	221 ± 11.5	170.8 ± 9.7	50.2 ± 4.7	9
PI3K (CA)	432.3 ± 54.2	363.2 ± 49.5	69.2 ± 5.8	6
Ras (V12, C40)	359.2 ± 45.9	313.5 ± 44.2	45.6 ± 14.0	19
PTEN dsRNA	388.9 ± 55.9	315.5 ± 56.2	73.4 ± 17.9	17

3.3 *Alternation of somatic PI3K activity does not affect the rate of germ cell proliferation*

An increase in the rate of germline proliferations within a cyst, like the EGFR loss-of-function defect (Kiger *et al.* 2000), or a block in cyst differentiation could result in a higher germ/soma ratio and bloated tip phenotype as observed in the $Ras^{V12\ C40}$ and $PI3K^{CA}$ overexpressing backgrounds. To distinguish between the two possibilities, we stained the testes with anti-phosphorylated-Histone-3 (PH3) and separately estimated the germline mitotic indices (figure 3A–C). It revealed no significant difference with respect to the control, (figure 3D). Furthermore, we noticed that the apical part of the testes, expressing $PI3K^{CA}$ in the soma, was filled with germ cells containing enlarged nuclei with comparatively more dispersed chromatin (arrowheads, figure 3C). A similar experiment conducted in the $EGFR^{dsRNA}$ and $EGFR^{DN}$ backgrounds produced significant increase in the PH3 stained nuclei within each cyst (Gupta and Ray, unpublished). Also, the germ/soma ratios in these backgrounds were several folds higher than the wild-type. Hence, the above results ruled out a role for the somatic PI3K activity in regulating the germline divisions.

3.4 *Ectopic somatic activation of PI3K causes abnormal accumulation of spermatocytes at the premeiotic stage*

The somatic enclosure, marked by the anti-Armadillo staining (figure 4A and A′), appeared intact in the $PI3K^{DN}$, $PI3K^{CA}$, and $Ras^{V12,\ C40}$ overexpression backgrounds (figure 4B–D). To identify the somatic effects of PI3K activity on the rate of germline development, we estimated the stage-specific distribution of cysts in these backgrounds. In the $PI3K^{DN}$ background, the number of cysts at each spermatogonial stages, as well as the total number, were significantly reduced (figure 4E). The chromatin in the spermatocyte nuclei also appeared to decondense relatively closer to the testis apex (arrow, figure 4B). The gain of PI3K activity ($PI3K^{CA}$ and $Ras^{V12,\ C40}$ backgrounds), on the other hand, specifically enhanced the number of 16-cell, spermatogonial-stage cysts, which accumulated at the apical part of the testes, causing an abnormal bloating (figure 4C–E). Overexpression of $PI3K^{CA}$ caused a relatively greater accumulation as compared to the $Ras^{V12,\ C40}$. However, the proportional distribution of the cysts in the one- to eight-cell stages remained unaltered (figure 4F). Thus, it suggested that the cyst development up to the eight-cell stage would be unaffected in all these backgrounds. In comparison, a balance in the somatic PI3K activity would be critical for the germ cell differentiation particularly after the completion of transit amplification divisions.

The expression of *bam* in spermatogonia starts after the second mitosis, reaches a critical threshold after the third and disappears after the fourth mitosis (Insco *et al.* 2009). It is regulated by TGFβ signalling in the germline cells (Schulz *et al.* 2004), and described as a necessary and sufficient factor for arresting the germline TA (Insco *et al.* 2009; Ohlstein and McKearin 1997). To compare the cyst development until the eight-cell stage, we monitored the distribution of *BampbmpGFP* expressing cysts in the $PI3K^{DN}$, $PI3K^{CA}$ and $PTEN^{dsRNA}$ backgrounds (figure 4G–J). Although there was a moderate increase in the number of two-cell stage cysts in the $PI3K^{DN}$ and the 16-cell cysts in the $PI3K^{CA}$ backgrounds, the total number of Bam-positive cysts were not significantly altered (figure 4K). The $PI3K^{CA}$ overexpression, though, significantly increased the number of 16-cell, Bam-positive cysts (figure 4K). The increase in the number of these cysts, however, was less compared to the total number of 16-cell cysts found at the testis apex. Although not extensively quantified, a similar result was obtained in the $PTEN^{dsRNA}$ background. The persistence of Bam-positive 16-cell cysts in the $PI3K^{CA}$ backgrounds suggested that the regulation of somatic PI3K activity is particularly essential for managing the transition to the pre-meiotic stage after the conclusion of transit amplification divisions.

To test this hypothesis further, we estimated the sizes of spermatogonial cells at different stages, and physical distance of partly decondensed S2 stage nuclei from the apical

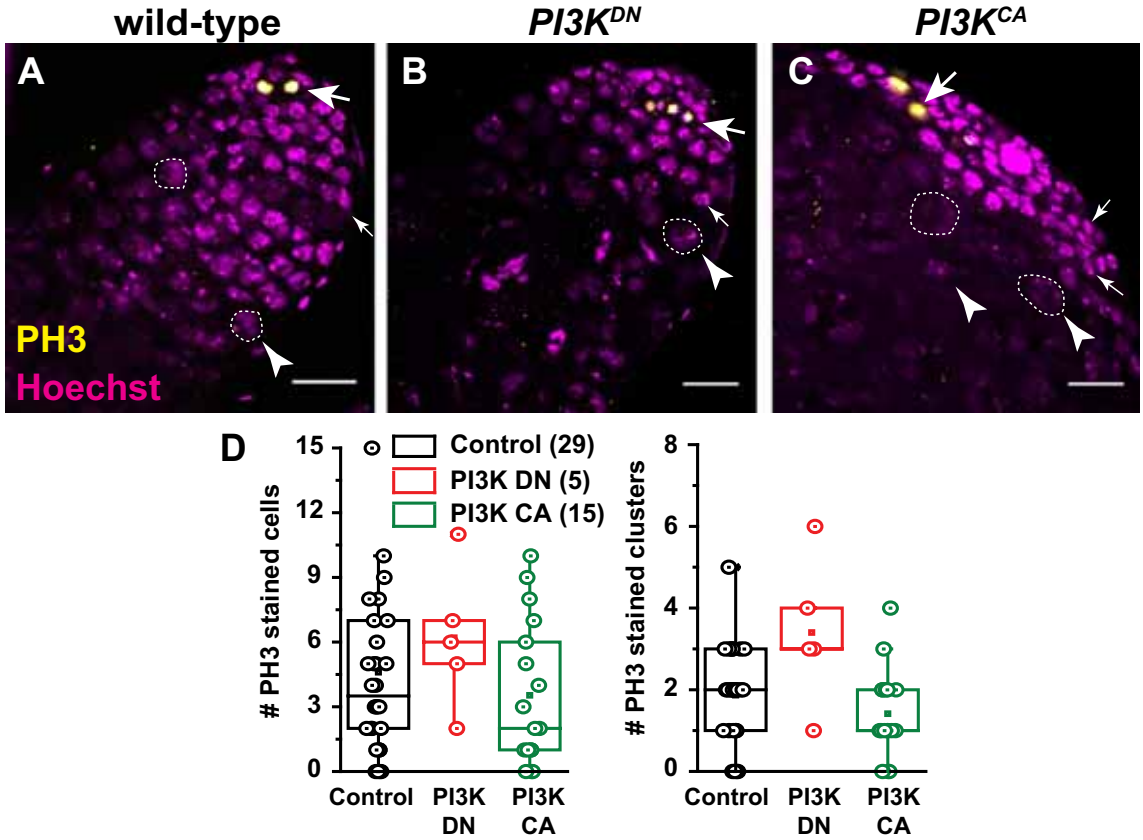

Figure 3. Estimation of germline mitotic indices in the backgrounds of altered somatic PI3K activity. Testes from *tjGal4; UAS-His2A-RFP/+* (**A**), *tjGal4 UAS-His2A-RFP/+*; *UAS-PI3K^{DN}/+* (**B**) and *tjGal4 UAS-His2A-RFP/+; UAS-PI3K^{CA}/+* (**C**) were immunostained with α-PH3 (yellow, arrow) and the Hoechst dye (magenta). Fine arrows indicate spermatogonial stage nuclei; arrowheads mark a few of the spermatocyte stage nuclei (also defined by dotted circles), and scale bars indicate 20 μm. (**D**) The box plots depict the number of PH3 stained cells in each testis from different genotypes (shown below each box). Each box shows the distribution of the 25–75% of data points with the median (dissecting bar) and the mean (central square) values marked on them.

tip (hub marked by FAS-III) and the Bam boundary, respectively, in *PI3K^{DN}* and *PI3K^{CA}* backgrounds. Even though the sizes of the germline cells in cysts at different stages were not altered in the *PI3K^{DN}* and *PI3K^{CA}* backgrounds (figure 4L), the cysts containing S2-like nuclei appeared significantly closer to the testis apex in the *PI3K^{DN}* background (figure 4M). Often, S3-like decondensed spermatocytes appeared adjacent to the Bam-expressing cysts (arrow, figure 4I). Therefore, it suggested that the somatic down-regulation of PI3K advances the rate of germline differentiation. The ectopic activation of PI3K in the soma resulted in the persistence of partly decondensed, post Bam-stage, spermatocyte nuclei, with the S2-like spermatocytes at a relatively greater distance away from the hub and Bam boundary (figure 4M). After the fourth mitosis, the germline cells undergo rapid G1-S transition and then get arrested in the G2 phase known as meiotic prophase (Cenci *et al.* 1994; Lindsley and Tokuyasu 1980). The chromatin decondensation in spermatocyte nuclei is considered to be a convenient indicator of the entry into the meiotic prophase (Lindsley and Tokuyasu 1980; McKee *et al.* 2012). The observation further suggested that down-regulation of the somatic PI3K activity could also play a critical role in regulating the transition to the spermatocyte stage.

3.5 *The somatic activation of PI3K suppresses spermatocyte arrest expression*

The expression and nuclear localization of several TATA-box Binding protein (TBF) associated factors (TAFs), such as the *spermatocyte-arrest* (*sa*) in the germline cells (figure 5A), marks this transition at the 16-cell stage (Chen *et al.* 2005). The TAFs also interact with the Polycomb group of proteins to modify the chromatin organization through targeted histone modification which enables the

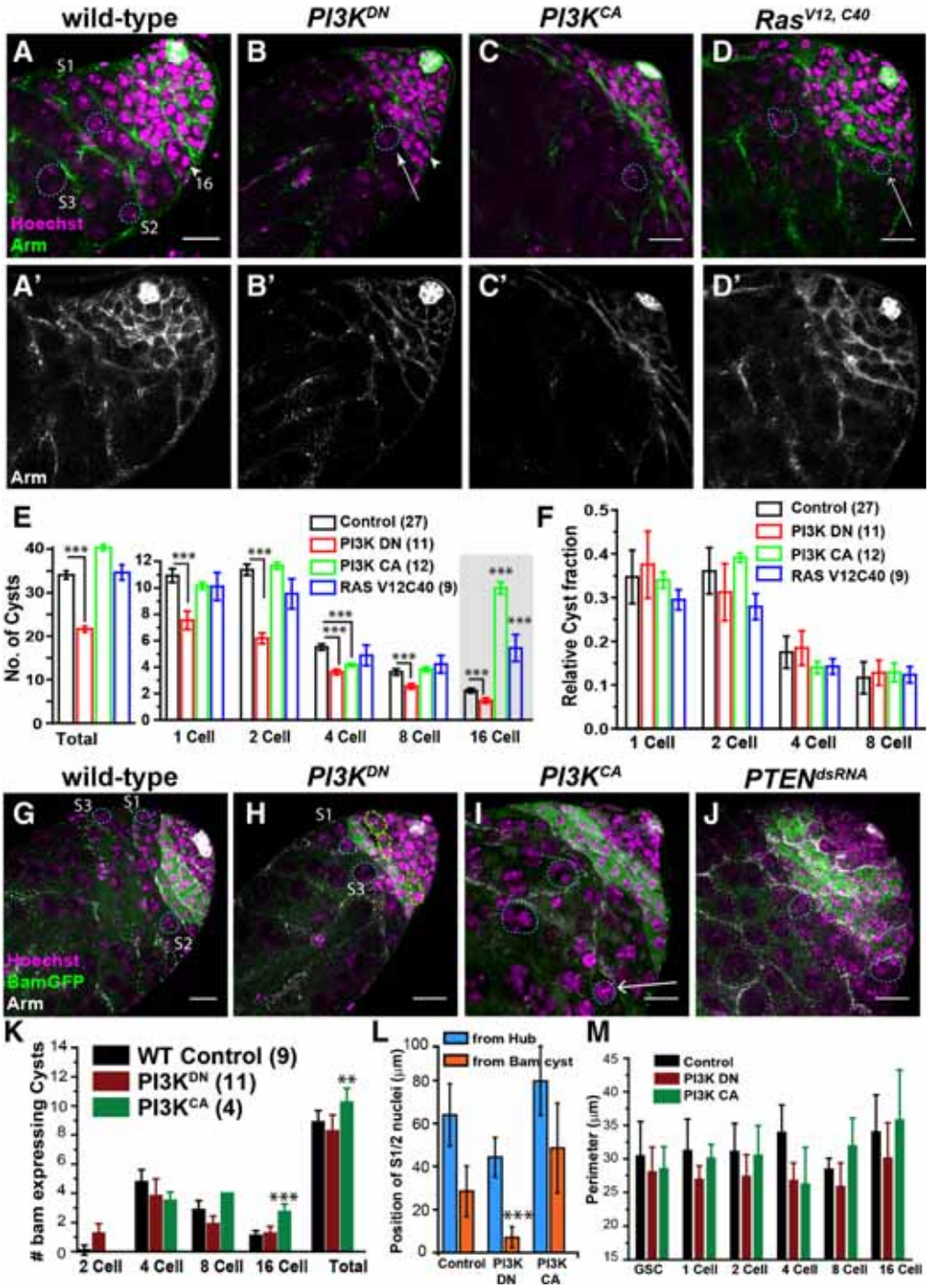

Figure 4. A quantitative analysis of the role of somatic PI3K activity in the germline differentiation. Testes from wild-type control (**A**), *PI3K*^{DN} (**B**), *PI3K*^{CA} (**C**), and *Ras*^{V12C40} (**D**) backgrounds were immunostained with anti-Armadillo (white) (**A′**–**D′**) marking the cyst boundary and Hoechst (magenta). (**E**, **F**) Histograms depict the stage-specific distribution of spermatogonial cysts, and relative cyst distribution on the total number of 1–8 cell stage cysts. *BamPbamGFP* expression in the wild-type control (**G**), *PI3K*^{DN} (**H**), *PI3K*^{CA} (**I**), and *PTEN*^{dsRNA} (**J**) backgrounds. The yellow dotted circle indicates condensed TA nuclei and blue dotted circle indicate decondensed nuclei which appear after the termination of *bam* expression. (**K**) Histograms depict average *bam*-expressing cysts in different genotypic backgrounds. (**L**) Histograms depict average distance of decondensed nuclei from Hub (red) and bam expressing cyst (green) in μm. (**M**) Histograms depict perimeter of germ cell in μm across spermatogonial stages. Scale bars indicate 20 μm. All error bars depict ±SD. The pair-wise significance of differences (p-values, *<0.05, **<0.01, and *** <0.001) relative to appropriate wild-type controls were calculated using Mann-Whitney μ-test.

G2/M transition during meiosis-I (Lin *et al.* 1996). The boundary of *sa-mCD8-GFP* expressing zone appeared relatively sharper and closer to the testis apex in the $PI3K^{DN}$ background (arrow, figure 5B′), whereas the boundary appeared more diffused in the $PI3K^{CA}$ background (arrows, figure 5C–C′). Also, a visibly large number of germ cells, most of them having a condensed chromatin (arrowheads, figure 5C), accumulated before the *sa-mCD8GFP* boundary. Interestingly, *tj* expression in somatic cyst cells stopped before the onset of the *sa* expression. Hence, the $PI3K^{CA}$ overexpression defect may suggest that downregulation of the somatic PI3K activity after the transit amplification stage is essential for triggering the meiotic prophase.

The Golgi dynamics have been shown to undergo changes during mitosis-meiosis transition and during the cell cycle phases (Payne and Schatten 2003). We used the Wheat Germ Agglutinin-RITC (WGA) staining assay, to assess the morphology of Golgi compartments in the germline cells. It stained a puncta and perinuclear structure in the spermatogonial cells (arrowheads and fine arrows, figure 5D–D′). The perinuclear staining was more prominent in the spermatocyte stages (yellow arrows, figure 5D–D′). In the $PI3K^{DN}$ background, the perinuclear staining in the spermatogonial stages was comparatively less pronounced and the large spermatocytes with strong perinuclear staining appeared relatively closer to the hub (figure 5E). In the $PI3K^{CA}$ background, even the spermatogonial cells close to the hub had a relatively high perinuclear WGA staining (fine arrows, figure 5F). Also, intense punctate staining was observed in cells closer to apical tip of testis upon ectopic activation of PI3K (arrowheads, figure 5F). WGA stains medial and trans-Golgi elements which accumulate in cells at the resting phase (Tartakoff and Vassalli 1983). The ribbon of the perinuclear Golgi complex is fragmented before G2/M transition (Wei and Seemann 2010; Corda *et al*. 2012). Therefore, intense perinuclear WGA staining could suggest that the spermatogonial divisions have relatively longer prophase in the $PI3K^{CA}$ background.

4. Discussion

4.1 *Somatic PI3K activity could regulate the rates of spermatogonial divisions*

The PI3K/Akt/mTOR pathway regulates the cell growth and homeostasis. PI3K is activated downstream due to the signalling through a large number of G-protein coupled receptors and insulin-like growth factor receptors regulating cell growth and proliferation (Whites and Kahn 1994; Murga *et al*. 1998; Engelman *et al*. 2006). EGFR and PI3K are also coactivated in gliomas (Read *et al*. 2009). Prior studies in *Drosophila* have revealed highly regulated PI3K activity in the wing, leg and haltere discs which maintain appropriate cell size and numbers (Leevers *et al*. 1996). However, its effect on the germline maintenance was unknown.

Here, we showed that the modulation of the somatic PI3K activity is unlikely to disrupt the transit amplification divisions. The somatic downregulation of PI3K significantly reduced the number of cysts at all stages and advanced the *bam* expression without affecting the stage-specific cyst distribution. The sizes of germline cells at all stages were comparable to the wild-type control. Hence, we concluded that the loss of PI3K activity advances the rate of cell divisions during the transit amplification stages. The conjecture is consistent with the somatic overactivation of PI3K which caused accumulation of the spermatogonial cells with prominent perinuclear Golgi, and the 16-cell cysts bearing partly decondensed nuclei, resembling the S1 and S2 stages. Together, these observations suggested that a balance of PI3K activity in the somatic cyst cells may control the rate of germline divisions and differentiation during the spermatogonial stages. A similar result was obtained by somatic overexpression of $EGFR^{CA}$ earlier (Hudson *et al.* 2013).

$Ras^{V12,\ C40}$ selectively activates the PI3K *in vivo* (Karim and Rubin 1998; Halfar *et al*. 2001), and PTEN moderated the PI3K-depednent signalling downstream through PI(3,4,5)P de-phosphorylation (Lee *et al*. 1999). Hence, one expected a similar phenotype in all three cases. Although the phenotypes have gross morphological similarities, we found distinct quantitative differences. Therefore, it is plausible that the ectopic activation of PI3K targets additional downstream components that are not regulated through the inositide signalling.

4.2 *The somatic PI3K activity could influence the onset of meiotic prophase*

Spermatogonia to spermatocyte transition are accompanied with relatively long meiotic prophase in germline cells. During this period, the transcriptional and translational activities increase substantially in the germ cells which continue to grow. The initiation of the spermatocyte stage is associated with rapid chromatin decondensation which also coincided with the increase in transcriptional activities. This spermatocyte-specific transcription is carried out by two major protein families, the testis meiotic arrest complex (tMAC), and the testis-specific TATA-binding protein (TBP) associated Factors (tTAFs) (Lin *et al.* 1996; White-Cooper *et al.* 1998) such as the SA. Mutations in the genes expressing tMACs and tTAFs invariably result in a differentiation arrest at meiosis-I. Here we showed that the somatic upregulation of PI3K activity led to a delayed expression of *sa* with concomitant accumulation of the cysts carrying S1/2 stage spermatocytes. We used the *tjGal4* driver that

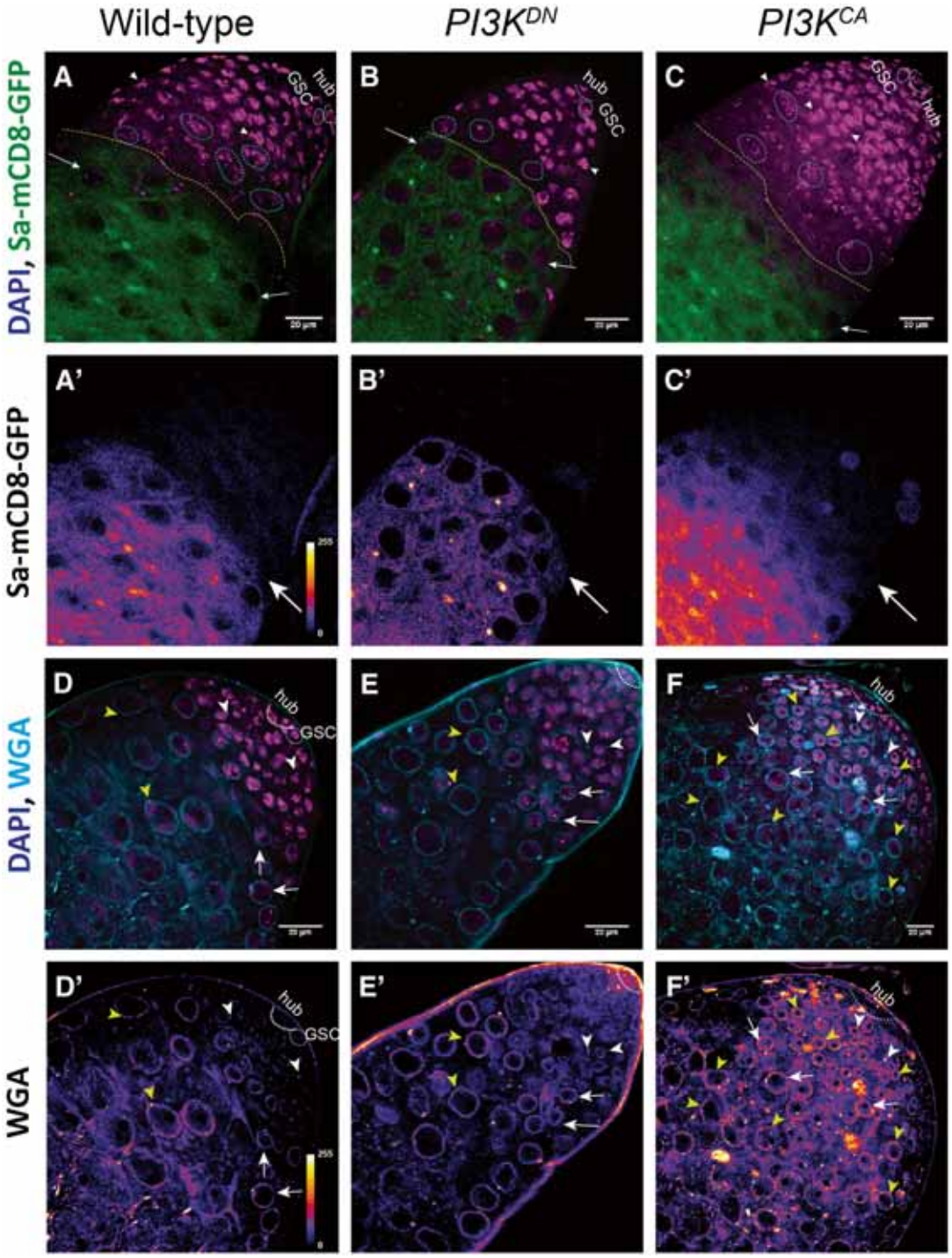

Figure 5. Somatic PI3K activity regulates spermatogonial differentiation. sa-CD8GFP expression in wild-type control (**A**), $PI3K^{DN}$ (**B**) and $PI3K^{CA}$ (**C**) backgrounds depicts the onset of spermatocyte stages. White Arrowhead indicate condensed TA zone nuclei; white arrow indicates decondensed spermatocyte nuclei. Broken blue circle indicate decondensed 16-cell nuclei. The broken yellow line marks the boundary between the spermatogonial and spermatocyte (green) stage cysts. Note that the sa-mCD8GFP level is visibly lowered in the $PI3K^{CA}$ background (**A′**, **C′**), and decondensed nuclei appear before sa expression. Wheat germ agglutinin staining for total Golgi content in wild-type control (**D**), $PI3K^{DN}$ (**E**) and $PI3K^{CA}$ (**F**) backgrounds reveal arrest in early germ cell divisions. White arrowhead indicates punctate WGA staining and yellow arrowhead point to intense perinuclear WGA stain. The white arrow indicates decondensed cell nuclei. Scale bars indicate 20 μm.

expresses until the *sa* expression stage in wild-type, to express the PI3K modifiers. Therefore, the effect observed was limited to the spermatogonia and early spermatocyte stages. It also helped to highlight the role of the somatic PI3K activity at the transition stage.

The inositide signalling regulates a vast range of metabolic activities including the mitochondrial activation and glucose utilization pathways within a cell. Preliminary studies in the somatic modification of Akt and mTORC1 activities indicated that the PI3K role in the germline differentiation might be independent of its metabolic functions (Gupta and Ray, unpublished). Independent dye permeability tests suggested that the somatic encapsulation of the germline cells become tighter during the 16-cell stage due to the formation of septate junctions between the cyst cells (Fairchild *et al.* 2015). Disruption of the septate junctions increased the dye permeation and arrested the germ cell differentiation. Dlg1 also plays an important role in the septate junction assembly and cyst encapsulation (Papagiannouli and Mechler 2009). In addition, the Dlg1 and PI3K activities were found to control the nephron progenitor population in kidney (Ahn *et al.* 2013). The membrane localization of PTEN and PI3K activation is regulated by PDZ-domain-containing, MAGUK family of proteins, such as the Dlg1 (Wu *et al.* 2000a, b; Kumar *et al.* 2014). Also, the PI3K pathway is implicated in the establishment of cell polarity by regulating Myosin-II localization in cultured cells (Chung *et al.* 2001). Hence, the cyst encapsulation may downregulate PI3K-depepdent signalling in the somatic cyst cells and promote the feedback signal facilitating the neighboring germ cell differentiation.

Acknowledgements

We thank Kenneth Irvine, Dorothea Godt, the Bloomington Stock Center, Vienna Drosophila Resource Center, and Developmental Studies Hybridoma Bank, Iowa, USA, for the fly stocks and other reagents. We also acknowledge Prakash Joti for experimental support. The project is supported by an intramural fund of TIFR, Department of Atomic Energy, and by the DBT Grant BT/PR/4585/Med/31/155/2012 Dtd. 28/09/2012.

References

Ahn S-Y, Kim Y, Kim ST, Swat W and Miner JH 2013 Scaffolding proteins DLG1 and CASK cooperate to maintain the nephron progenitor population during kidney development. *J. Am. Soc. Nephrol.* **24** 1127–1138

Biteau B, Hochmuth CE and Jasper H 2011 Maintaining tissue homeostasis: dynamic control of somatic stem cell activity. *Cell Stem Cell* **9** 402–411

Breuhahn K, Longerich T and Schirmacher P 2006 Dysregulation of growth factor signaling in human hepatocellular carcinoma. *Oncogene* **25** 3787–3800

Cenci G, Bonaccorsi S, Pisano C, Verni F and Gatti M 1994 Chromatin and microtubule organization during premeiotic, meiotic and early postmeiotic stages of Drosophila melanogaster spermatogenesis. *J. Cell Sci*. 3521–34

Chen X, Hiller M, Sancak Y and Fuller MT 2005 Tissue-specific TAFs counteract polycomb to turn on terminal differentiation. *Science* **310** 869–872

Chung CY, Potikyan G and Firtel RA 2001 Control of cell polarity and chemotaxis by Akt/PKB and PI3 kinase through the regulation of PAKa. *Mol. Cell* **7** 937–947

Corda D, Barretta ML, Cervigni RI and Colanzi A 2012 Golgi complex fragmentation in G2/M transition: an organelle-based cell-cycle checkpoint. *IUBMB Life* **64** 661–670

Davies EL and Fuller MT 2008 Regulation of self-renewal and differentiation in adult stem cell lineages: lessons from the drosophila male germ line. *Cold Spring Harb. Symp. Quant. Biol.* **73** 137–145

Duan H, Qu L and Shou C 2014 Activation of EGFR-PI3K-AKT signaling is required for Mycoplasma hyorhinis-promoted gastric cancer cell migration. *Cancer Cell Int.* **14** 135

Engelman JA, Luo J and Cantley LC 2006 The evolution of phosphatidylinositol 3-kinases as regulators of growth and metabolism. *Nat. Rev. Genet.* **7** 606–619

Fairchild MJ, Smendziuk CM and Tanentzapf G 2015 A somatic permeability barrier around the germline is essential for Drosophila spermatogenesis. *Development* **142** 268–281

Ferreira A and Milán M 2015 Dally proteoglycan mediates the autonomous and nonautonomous effects on tissue growth caused by activation of the PI3K and TOR pathways. *PLoS Biol.* **13** e1002239

Fuller MT 1993 Spermatogenesis. *Dev. Drosoph. melanogaster.* **1** 71–147

Fuller MT 1998 Genetic control of cell proliferation and differentiation in Drosophila spermatogenesis. *Semin. Cell Dev. Biol.* **9** 433–444

Galagovsky D, Katz MJ, Acevedo JM, Sorianello E, Glavic A and Wappner P 2014 The Drosophila insulin-degrading enzyme restricts growth by modulating the PI3K pathway in a cell-autonomous manner. *Mol. Biol. Cell* **25** 916–924

Gao S and Liu Y 2012 Intercepting noncoding messages between germline and soma. *Genes Dev.* **26** 1774–1779

Gönczy P, Matunis E and DiNardo S 1997 bag-of-marbles and benign gonial cell neoplasm act in the germline to restrict proliferation during Drosophila spermatogenesis. *Development* **124** 4361–4371

Halfar K, Rommel C, Stocker H and Hafen E 2001 Ras controls growth, survival and differentiation in the Drosophila eye by different thresholds of MAP kinase activity. *Development* **128** 1687–1696

Hardy RW, Tokuyasu KT, Lindsley DL and Garavito M 1979 The germinal proliferation center in the testis of Drosophila melanogaster. *J. Ultrastruct. Res.* **69** 180–190

Hudson AG, Parrott BB, Qian Y and Schulz C 2013 A temporal signature of epidermal growth factor signaling regulates the

differentiation of germline cells in testes of Drosophila melanogaster. *PLoS One* **8** e70678

Ibar C, Cataldo VF, Vásquez-Doorman C, Olguín P and Glavic A 2013 Drosophila p53-related protein kinase is required for PI3K/-TOR pathway-dependent growth. *Development* **140** 1282–1291

Insco ML, Leon A, Tam CH, McKearin DM and Fuller MT 2009 Accumulation of a differentiation regulator specifies transit amplifying division number in an adult stem cell lineage. *Proc. Natl. Acad. Sci. USA* **106** 22311–22316

Joti P, Ghosh-Roy A and Ray K 2011 Dynein light chain 1 functions in somatic cyst cells regulate spermatogonial divisions in Drosophila. *Sci. Rep.* **1** 173

Karim FD and Rubin GM 1998 Ectopic expression of activated Ras1 induces hyperplastic growth and increased cell death in Drosophila imaginal tissues. *Development* **125** 1–9

Kasahara K, Goto H, Izawa I, Kiyono T, Watanabe N, Elowe S, Nigg EA and Inagaki M 2013 PI 3-kinase-dependent phosphorylation of Plk1-Ser99 promotes association with 14-3-3γ and is required for metaphase-anaphase transition. *Nat. Commun.* **4** 1882

Kiger AA, White-Cooper H and Fuller MT 2000 Somatic support cells restrict germline stem cell self-renewal and promote differentiation. *Nature* **407** 750–754

Kumar M, Kong K and Javier RT 2014 Hijacking Dlg1 for oncogenic phosphatidylinositol 3-kinase activation in human epithelial cells is a conserved mechanism of human adenovirus E4-ORF1 proteins. *J. Virol.* **88** 14268–14277

Kusumi N, Watanabe M, Yamada H, Li S-A, Kashiwakura Y, Matsukawa T, Nagai A, Nasu Y, *et al*. 2007 Implication of amphiphysin 1 and dynamin 2 in tubulobulbar complex formation and spermatid release. *Cell Struct. Funct.* **32** 101–113

Lee J-O, Yang H, Georgescu M-M, Di Cristofano A, Maehama T, Shi Y, Dixon JE, Pandolfi P, *et al*. 1999 Crystal structure of the PTEN tumor suppressor. *Cell* **99** 323–334

Leevers SJ, Weinkove D, MacDougall LK, Hafen E and Waterfield MD 1996 The Drosophila phosphoinositide 3-kinase Dp110 promotes cell growth. *EMBO J.* **15** 6584–6594

Li MA, Alls JD, Avancini RM, Koo K and Godt D 2003 The large Maf factor traffic jam controls gonad morphogenesis in Drosophila. *Nat. Cell Biol.* **5** 994–1000

Li Y, Minor NT, Park JK, McKearin DM and Maines JZ 2009 Bam and Bgcn antagonize Nanos-dependent germ-line stem cell maintenance. *Proc. Natl. Acad. Sci. USA* **106** 9304–9309

Lim JGY and Fuller MT 2012 Somatic cell lineage is required for differentiation and not maintenance of germline stem cells in Drosophila testes. *Proc. Natl. Acad. Sci. USA* **109** 18477–18481

Lin TY, Viswanathan S, Wood C, Wilson PG, Wolf N and Fuller MT 1996 Coordinate developmental control of the meiotic cell cycle and spermatid differentiation in Drosophila males. *Development* **122** 1331–1341

Lindsley DT and Tokuyasu KT 1980 Spermatogenesis. In: Ashburner M, Wright TRF (eds) *The Genetics and Biology of Drosophila*, Vol. 2d. 225–294

McKee BD, Yan R and Tsai J-H 2012 Meiosis in male Drosophila. *Spermatogenesis* **2** 167–184

Murga C, Laguinge L, Wetzker R, Cuadrado A and Gutkind JS 1998 Activation of Akt/protein kinase B by G protein-coupled receptors: a role for and subunits of heterotrimeric g proteins acting through phosphatidylinositol-3-OH kinase. *J. Biol. Chem.* **273** 19080–19085

Ohlstein B and McKearin D 1997 Ectopic expression of the Drosophila Bam protein eliminates oogenic germline stem cells. *Development* **124** 3651–3662

Papagiannouli F and Mechler BM 2009 discs large regulates somatic cyst cell survival and expansion in Drosophila testis. *Cell Res.* **19** 1139–1149

Payne C and Schatten G 2003 Golgi dynamics during meiosis are distinct from mitosis and are coupled to endoplasmic reticulum dynamics until fertilization. *Dev. Biol.* **264** 50–63

Read RD, Cavenee WK, Furnari FB and Thomas JB 2009 A drosophila model for EGFR-Ras and PI3K-dependent human glioma. *PLoS Genet.* **5** e1000374

Salony S, Alves X, Dey-Guha CP, Ritsma I, Boukhali L, Lee M, Chowdhury JH, Ross J, *et al*. 2016 AKT inhibition promotes nonautonomous cancer cell survival. *Mol. Cancer Ther.* **15** 142–153

Schulz C, Kiger AA, Tazuke SI, Yamashita YM, Pantalena-Filho LC, Jones DL, Wood CG and Fuller MT 2004 A misexpression screen reveals effects of bag-of-marbles and TGF beta class signaling on the Drosophila male germ-line stem cell lineage. *Genetics* **167** 707–723

Soler A, Angulo-Urarte A and Graupera M 2015 PI3K at the crossroads of tumor angiogenesis signaling pathways. *Mol. Cell. Oncol.* **2** e975624

Tartakoff AM and Vassalli P 1983 Lectin-binding sites as markers of Golgi subcompartments: proximal-to-distal maturation of oligosaccharides. *J. Cell Biol.* **97** 1243–1248

Tétreault M-P, Chailler P, Beaulieu J-F, Rivard N and Ménard D 2008 Epidermal growth factor receptor-dependent PI3K-activation promotes restitution of wounded human gastric epithelial monolayers. *J. Cell. Physiol.* **214** 545–557

Toulany M, Baumann M and Rodemann HP 2007 Stimulated PI3K-AKT signaling mediated through ligand or radiation-induced EGFR depends indirectly, but not directly, on constitutive K-Ras activity. *Mol. Cancer Res.* **5** 863–872

Tran J, Brenner TJ and DiNardo S 2000 Somatic control over the germline stem cell lineage during Drosophila spermatogenesis. *Nature* **407** 754–757

Wei J-H and Seemann J 2010 Unraveling the Golgi ribbon. *Traffic* **11** 1391–1400

Weinkove D, Neufeld TP, Twardzik T, Waterfield MD and Leevers SJ 1999 Regulation of imaginal disc cell size, cell number and organ size by Drosophila class I(A) phosphoinositide 3-kinase and its adaptor. *Curr. Biol.* **9** 1019–1029

White-Cooper H, Schafer MA, Alphey LS and Fuller MT 1998 Transcriptional and post-transcriptional control mechanisms coordinate the onset of spermatid differentiation with meiosis I in Drosophila. *Development.* **125** 125–134

Whites MF and Kahn CR 1994 The insulin signaling system*. *J. Biol. Chem.* **269** 1–4

Wu MY and Hill CS 2009 TGF-β superfamily signaling in embryonic development and homeostasis. *Dev. Cell.* **16** 329–343

Wu X, Hepner K, Castelino-Prabhu S, Do D, Kaye MB, Yuan XJ, Wood J, Ross C, *et al*. 2000a Evidence for regulation of the PTEN tumor suppressor by a membrane-localized multi-PDZ domain containing scaffold protein MAGI-2. *Proc. Natl. Acad. Sci. USA* **97** 4233–4238

Wu Y, Dowbenko D, Spencer S, Laura R, Lee J, Gu Q and Lasky LA 2000b Interaction of the tumor suppressor PTEN/MMAC with a PDZ domain of MAGI3, a novel membrane-associated guanylate kinase. *J. Biol. Chem.* **275** 21477–21485

Xi X, Tatei K, Kihara Y and Izumi T 2014 Expression pattern of class I phosphoinositide 3-kinase and distribution of its product, phosphatidylinositol-3,4,5-trisphosphate, during Drosophila embryogenesis. *Gene Expr. Patterns* **15** 88–95

Zoller R and Schulz C 2012 The Drosophila cyst stem cell lineage. *Spermatogenesis* **2** 145–157

MS received 08 September 2016; accepted 14 February 2017

Corresponding editor: SUBHASH C LAKHOTIA